Yuan *et al. Biochar* (2026) 8:147
https://doi.org/10.1007/s42773-026-00658-0

Biochar

ORIGINAL RESEARCH Open Access

Persistent free radicals on biochar surfaces redirect straw-derived carbon toward mineral-associated organic matter

Dan Yuan[1], Jiao Yuan[1,2], Xiangxiang Hao[3], Xinliang Dong[1*], Ping Wu[1], Yuming Zhang[1], Zhenhua Yu[3] and Shuping Qin[1*]

Abstract

Returning crop residues to soil is a central strategy for increasing soil organic carbon (SOC), yet whether biochar-associated persistent free radicals (PFRs) actively regulate the stabilization of residue-derived carbon remains unresolved. Here, graded PFR activities were generated by selective radical quenching while maintaining similar biochar physicochemical properties, and ^{13}C-labeled straw was used to trace residue-derived carbon dynamics in two contrasting agricultural soils. Biochar PFRs enhanced hydroxyl radical (·OH) production in a dose-dependent manner, with the highest-PFR treatment generating 6.1- and 18.1-fold higher ·OH levels than the straw-only control in black soil and fluvo-aquic soil, respectively. This abiotic oxidation accelerated early-stage (0–14 d) straw carbon mineralization without increasing net carbon loss. Instead, it redirected straw-derived carbon toward aromatic intermediates that preferentially accumulated as mineral-associated organic matter (MAOM), increasing the proportion of MAOM carbon derived from straw from 59.4% to 64.2% in black soil and from 53.8% to 60.0% in fluvo-aquic soil. Structural equation modeling further demonstrated that PFRs promoted MAOM formation primarily through ·OH-driven chemical transformation, whereas microbial communities acted mainly as secondary responders. These findings demonstrate that biochar-derived PFRs redirect, rather than simply accelerate, straw-derived carbon turnover by coupling abiotic oxidation with microbial processing. This study establishes a mechanistic link between biochar surface redox chemistry and soil carbon persistence, providing a mechanistic basis for designing biochars with enhanced carbon sequestration potential.

Highlights

- Biochar persistent free radicals initiate abiotic oxidation of straw-derived carbon.
- PFR-driven chemical transformation redirects residue carbon into mineral-associated pools.
- Coupled abiotic–biotic pathways explain biochar-induced straw carbon stabilization.

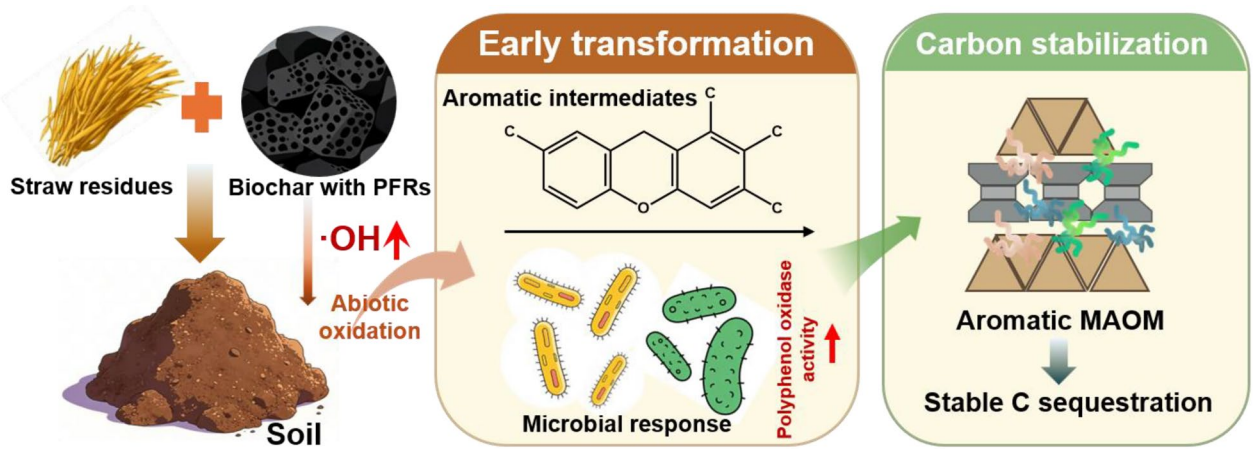
Keywords Soil organic carbon, Biochar, Persistent free radicals (PFRs), Mineral-associated organic matter (MAOM), Abiotic oxidation, Microbial community function

*Correspondence:
Xinliang Dong
xldong@sjziam.ac.cn
Shuping Qin
qinshuping@sjziam.ac.cn
Full list of author information is available at the end of the article

© The Author(s) 2026. **Open Access** This article is licensed under a Creative Commons Attribution 4.0 International License, which permits use, sharing, adaptation, distribution and reproduction in any medium or format, as long as you give appropriate credit to the original author(s) and the source, provide a link to the Creative Commons licence, and indicate if changes were made. The images or other third party material in this article are included in the article's Creative Commons licence, unless indicated otherwise in a credit line to the material. If material is not included in the article's Creative Commons licence and your intended use is not permitted by statutory regulation or exceeds the permitted use, you will need to obtain permission directly from the copyright holder. To view a copy of this licence, visit http://creativecommons.org/licenses/by/4.0/.

Springer

Graphical Abstract



1 Introduction

Soil organic matter (SOM) represents the largest actively cycling carbon reservoir in terrestrial ecosystems. Small changes in its size can exert disproportionate effects on atmospheric CO_2 concentrations and climate regulation (Raza et al. 2024). Increasing soil organic carbon (SOC) stocks through agricultural management is therefore widely recognized as a key strategy for climate change mitigation while sustaining soil fertility and productivity (Nazir et al. 2024; Shi and Xia 2024). Returning crop residues to soil is the most widely implemented practice, directly reintegrating photosynthetically fixed carbon into the soil system (Karan et al. 2023; Xu et al. 2024). However, residue-derived carbon is highly dynamic, and a large fraction is rapidly mineralized following incorporation. More than half of residue carbon can be lost as CO_2 within the first year, substantially limiting the long-term contribution of residue return to SOC accumulation (Alvarez 2024; Khan et al. 2022; Lenka et al. 2019). Identifying mechanisms that redirect residue-derived carbon toward persistent soil carbon pools remains a central challenge in soil carbon research.

Co-application of biochar with crop residues has emerged as a promising strategy to enhance soil carbon retention. Biochar contains condensed aromatic structures that are intrinsically resistant to microbial decomposition and can persist in soils for centuries, directly contributing to stable SOC pools (Chang et al. 2022; Chen et al. 2021). In addition, biochar can indirectly promote carbon stabilization by sorbing dissolved organic compounds, providing microhabitats, and facilitating organic–mineral associations (Ma et al. 2023; Tang et al. 2025; Weng et al. 2022). Despite these well-documented effects, most explanations emphasize biochar's physical structure or bulk chemical composition, treating biochar largely as a passive amendment. Such perspectives provide limited insight into how biochar actively regulates the transformation pathways of fresh organic inputs.

An increasingly recognized property of biochar is the presence of persistent free radicals (PFRs), which have recently emerged as one of the most important redox-active components governing the environmental reactivity of biochar (Chen et al. 2025; Ruan et al. 2019). Recent studies have demonstrated that biochar-derived PFRs can mediate extracellular electron transfer and continuously activate molecular oxygen to generate reactive oxygen species (ROS), particularly hydroxyl radical (·OH) (Tang et al. 2021; Tao et al. 2022), thereby extending the role of biochar beyond passive carbon storage to active regulation of redox reactions. Increasing evidence further suggests that ROS-mediated oxidation can substantially alter the molecular composition of natural organic matter, promote aromatization and humification, and regulate soil carbon turnover (Dong et al. 2025; Fang et al. 2025; Yang et al. 2025a, b). Although these findings imply that biochar-derived PFRs may actively participate in soil carbon cycling, current knowledge primarily focuses on contaminant degradation, dissolved organic matter oxidation, or mechanistic reviews, whereas their direct role in regulating the transformation and stabilization of fresh residue-derived carbon in soils remains largely unexplored.

Biochar is widely recognized as an effective strategy for enhancing soil carbon sequestration, but its influence on residue-derived carbon transformation remains controversial. Some studies have reported that biochar

accelerates the mineralization of residue-derived or native soil carbon by stimulating microbial activity and oxidative processes (Lu et al. 2022), whereas others have shown enhanced carbon stabilization through increased MAOM formation and organo–mineral associations (Wang et al. 2026). These apparently conflicting observations suggest that biochar may simultaneously stimulate early carbon turnover and long-term carbon stabilization, yet the mechanism underlying this apparent paradox remains unresolved. One major reason for these inconsistencies is that previous studies have generally compared biochars differing simultaneously in surface area, mineral composition, oxygen-containing functional groups, and PFR abundance, making it difficult to distinguish the specific contribution of PFRs (Chacón et al. 2020; Fuertes et al. 2010; Li et al. 2020a; Wang et al. 2022).

Here, we selectively manipulated PFR activity on biochar from a single feedstock using chemical quenching while minimizing changes in other physicochemical properties, and tested the proposed mechanism in two contrasting agricultural soils differing in pH and native SOC. Using ^{13}C-labeled straw together with ROS quantification, DOM spectroscopy, microbial community analysis, and structural equation modeling, we directly disentangled abiotic and biotic pathways controlling straw-derived carbon transformation. This experimental design enables direct evaluation of the specific contribution of PFRs to residue-derived carbon stabilization, thereby providing a mechanistic explanation for the long-standing paradox that biochar can simultaneously accelerate early carbon transformation while enhancing long-term carbon stabilization. Our findings establish a mechanistic link between biochar surface redox chemistry and soil carbon persistence, providing a theoretical basis for the rational design of biochars that maximize long-term SOC stabilization.

2 Materials and methods

2.1 Soils and experimental materials

2.1.1 Soil collection and pre-treatment

Surface soils (0–20 cm) were collected from two representative agricultural regions in China. A black soil (Pachic Haploboroll, USDA Soil Taxonomy) (Soil Survey Staff 2010) was sampled from the Hailun Agricultural Ecological Experimental Station, Heilongjiang Province (126°38′E, 47°26′N), characterized by high organic carbon content and well-developed structure (SOC 28.5 ± 0.87 g kg^{-1}; pH 6.8 ± 0.08). A fluvo-aquic soil (Haplic Cambisol, WRB/FAO classification) (Mantel et al. 2023) was collected from the Luancheng Agricultural Ecosystem Experimental Station, Hebei Province (37°53′N, 114°41′E), representing an intensively managed soil with lower organic carbon content (SOC 12.3 ± 0.48 g kg^{-1}; pH 8.1 ± 0.11). These classifications follow the nomenclature convention used by the respective long-term experimental stations and previous studies (Hao et al. 2022; Qin et al. 2012). These two soils, both widely distributed in northern China, were selected for their contrasting pH and SOC contents to evaluate the generality of this mechanism and whether it is modulated by soil properties.

All soils were air-dried, gently crushed, passed through a 2-mm sieve to remove visible plant residues and stones, and stored at 4 °C prior to incubation. Soil physicochemical properties were determined as follows: soil pH was determined in a soil-to-water suspension (1:2.5, w/v) using a calibrated glass electrode; SOC was determined by the potassium dichromate oxidation–external heating method (Walkley–Black method).

2.1.2 ^{13}C-labeled straw and biochar preparation

Maize plants were cultivated in a controlled chamber continuously supplied with $^{13}CO_2$. After harvest, aboveground straw was oven-dried (60 °C), ground, and sieved (< 0.15 mm). The $\delta^{13}C$ value of labeled straw was + 450 ± 25‰.

Unlabeled maize straw was pyrolyzed at 500 °C for 2 h under an N_2 atmosphere to produce base biochar. The biochar was ground (< 0.15 mm), repeatedly washed with deionized water until pH stabilized, and dried at 60 °C. This material served as the unquenched biochar (BC-Q0).

2.1.3 Generation of graded PFR activity by chemical quenching

Persistent free radical (PFR) activity was selectively regulated using *L*-ascorbic acid as a radical scavenger. Biochar was reacted with *L*-ascorbic acid solutions (0, 20, 40, 60, 80, and 100 g L^{-1}) at a solid-to-liquid ratio of 1:10, shaken for 24 h at 25 °C in the dark. After reaction, suspensions were centrifuged (8,000 rpm) and washed repeatedly with deionized water until no residual ascorbic acid was detected in the supernatant by UV spectroscopy, thereby minimizing potential carryover of the quenching reagent into subsequent soil incubation experiments. Biochars were then dried (60 °C) and designated BC-Q0 to BC-Q100, forming a continuous gradient of decreasing PFR activity.

2.2 Incubation experiment design

A two-factor completely randomized design was employed, with soil type (black soil vs. fluvo-aquic soil) and biochar PFR level as factors. Treatments included straw-only controls (S) and straw amended with biochars differing in PFR activity (S + BC-Q0 to S + BC-Q100), each with four replicates.

Soils were pre-incubated for 7 days, then amended with ^{13}C-labeled straw (1% w/w) and biochar (2% w/w). Soil moisture was adjusted to 60% of water-holding capacity. Aliquots equivalent to 50 g dry soil were placed into 150 mL sealed incubation jars containing a vial with 5 mL of 1 M NaOH to trap CO_2. Jars were incubated at 25 °C in the dark. Destructive sampling was conducted on days 1, 3, 7, 14, 28, 56, and 84 to capture the rapid physicochemical and biological responses immediately following straw incorporation during the first 2 weeks, later sampling focused on the slower processes of organic matter transformation and residue-derived carbon stabilization (Cotrufo et al. 2015; Kallenbach et al. 2016).

2.3 Biochar characterization and PFRs determination

Elemental composition (C, O) was determined using an elemental analyzer (Elementar, Germany). Specific surface area was measured by N_2 adsorption at 77 K using a BET analyzer (ASAP 2460, Micromeritics, USA). Biochar PFRs were quantified by electron paramagnetic resonance (EPR) spectroscopy (Bruker ELEXSYS E500, Germany). Spin concentrations were calculated by double integration of EPR spectra relative to a calibrated standard, and g-factors were used to verify radical types (Text S1).

2.4 Analytical methods

2.4.1 Carbon mineralization and isotopic partitioning

CO_2 trapped in NaOH was precipitated with 0.5 M $BaCl_2$, and residual NaOH was titrated with 0.25 M HCl to determine cumulative CO_2 production. First-order mineralization rate constants (k) were estimated by fitting early-stage CO_2 release data to exponential decay models. For treatments, $\delta^{13}C$ values of CO_2 were measured using a GasBench II coupled to an isotope ratio mass spectrometer (IRMS), allowing quantification of straw-derived CO_2 based on isotopic mass balance (Text S2).

The contribution of straw-derived carbon to CO_2 emission and soil organic matter fractions was quantified using a two-endmember isotope mixing model:

$$f_{\text{straw}} = \frac{\delta^{13} C_{\text{sample}} - \delta^{13} C_{\text{soil}}}{\delta^{13} C_{\text{straw}} - \delta^{13} C_{\text{soil}}}$$

where f_{straw} represents the fraction of carbon derived from ^{13}C-labeled straw, and $\delta^{13}C$ values represent isotopic signatures of the measured sample, native SOC background, and labeled straw, respectively. The amount of straw-derived carbon in each physical fraction was calculated by multiplying f_{straw} by the total carbon content of that fraction. The percentage of straw-derived carbon in each fraction, including MAOM, represents the proportion of carbon within that fraction originating from the added ^{13}C-labeled straw.

2.4.2 Quantification of ·OH production

·OH production was quantified using the *p*-hydroxybenzoic acid (*p*-HBA) probe method. Fresh soil subsamples (1.0 g dry weight equivalent) were suspended in 10 mL phosphate buffer (10 mM, pH 7.0) containing 1.0 mM *p*-HBA and incubated at 25 °C for 1 h in the dark with gentle shaking (150 rpm). After incubation, suspensions were centrifuged (10,000×g, 10 min) and filtered (0.22 μm). Formation of 3,4-dihydroxybenzoic acid (3,4-DHBA) was quantified by HPLC with fluorescence detection (excitation 305 nm; emission 430 nm). External calibration with authentic standards was used, and ·OH production rates were calculated based on stoichiometric conversion. Probe-free controls were included to correct for background signals (Text S3).

2.4.3 Soil organic matter fractionation and chemical characterization

On day 84, soils were fractionated into free light fraction, microaggregate-occluded fraction, and mineral-associated organic matter (MAOM) using a combined density and particle-size fractionation method. Each fraction was freeze-dried and analyzed for total carbon and $\delta^{13}C$ using an elemental analyzer coupled to IRMS, allowing quantification of straw-derived carbon allocation. MAOM fractions were further analyzed by solid-state ^{13}C CP/MAS NMR spectroscopy. Aromatic carbon proportion was quantified by integrating the aromatic carbon resonance region (110–160 ppm) of the spectra and used as an indicator of oxidative chemical transformation.

2.4.4 Dissolved organic matter chemistry

Fresh soils were extracted with 0.5 M K_2SO_4, filtered (0.45 μm), and analyzed for dissolved organic carbon using a TOC analyzer. Specific ultraviolet absorbance at 254 nm ($SUVA_{254}$) was calculated as DOC-normalized absorbance and used as an index of DOM aromaticity and chemical transformation.

2.4.5 Microbial community and functional indicators

Total DNA was extracted from soils collected on day 84 for selected treatments. Bacterial 16S rRNA genes (V3–V4) and fungal ITS1 regions were amplified and sequenced on an Illumina MiSeq platform. Sequences were quality-filtered and taxonomically assigned using reference databases. Microbial functional responses were assessed using polyphenol oxidase activity as an indicator of oxidative enzyme associated with aromatic carbon processing (Text S4).

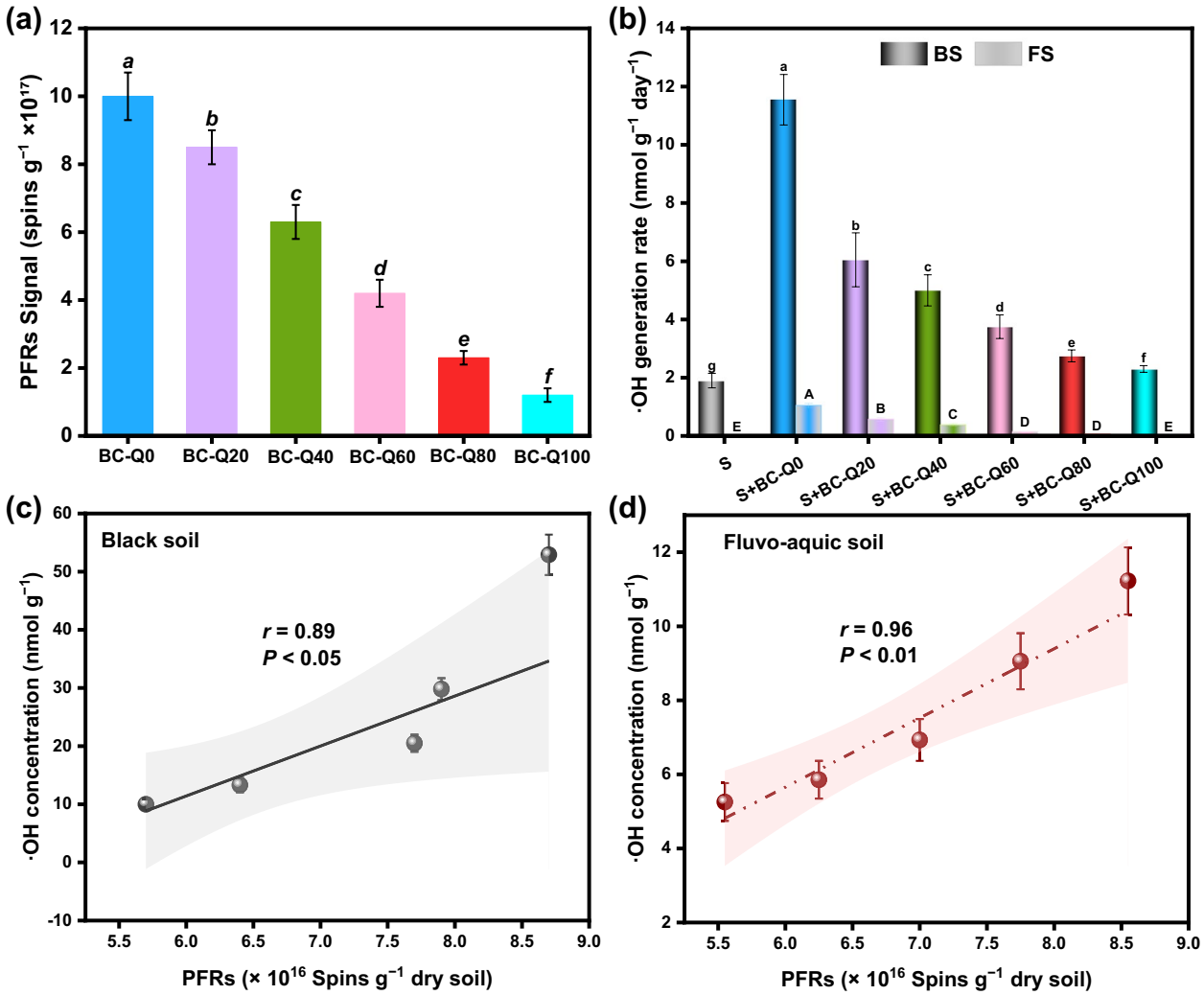


Fig. 1 Biochar persistent free radicals (PFRs) control hydroxyl radical (·OH) generation in soil. **a** EPR-determined PFR spin concentrations of biochars subjected to graded chemical quenching (BC-Q0 to BC-Q100). **b** ·OH generation rates in black soil (BS) and fluvo-aquic soil (FS) amended with biochars differing in PFR activity. **c**, **d** Linear relationships between biochar PFR concentration and ·OH production rate in black soil (**c**) and fluvo-aquic soil (**d**). Error bars represent standard deviations ($n = 4$)

2.5 Statistical analysis

Treatment effects were assessed using one-way ANOVA followed by Tukey's HSD test ($\alpha = 0.05$). Linear regression was used to evaluate dose–response relationships between PFRs, ·OH production, chemical transformation indicators, and MAOM-C. Structural equation modeling (SEM) was conducted using the lavaan package in R to quantify direct and indirect pathways linking PFRs, abiotic oxidation (·OH), chemical transformation ($SUVA_{254}$, MAOM chemistry), microbial functional indicators, and straw-derived MAOM stabilization.

3 Results

3.1 Establishment of graded PFR levels in biochars

Chemical quenching successfully regulated a continuous gradient of persistent free radical (PFR) intensities in biochars while preserving their core physicochemical properties. Electron paramagnetic resonance (EPR) spectra showed a decline in spin concentration from unquenched biochar (BC-Q0) to the most strongly quenched treatment (BC-Q100) (Fig. 1a). The PFR signal intensity of BC-Q100 was reduced to approximately 12% of that of BC-Q0.

Across treatments, specific surface area and elemental composition (C, H, and O contents) did not differ significantly (Table S1), confirming that the quenching

procedure selectively altered PFR abundance without modifying bulk biochar structure or chemistry.

3.2 PFR-dependent ·OH production and early straw carbon mineralization

Biochars differing in PFR activity induced distinct patterns of ·OH production during early incubation. In both black soil and fluvo-aquic soil, soils amended with high-PFR biochar (BC-Q0) exhibited significantly higher ·OH generation rates than straw-only controls and low-PFR biochar treatments (Fig. 1b). Across all soil treatments, ·OH production rates were positively correlated with EPR-determined PFR spin concentrations (black soil: $r=0.89$, $P<0.05$; fluvo-aquic soil: $r=0.96$, $P<0.01$) (Fig. 1c, d).

Consistent with enhanced abiotic reactivity, high-PFR biochar significantly increased the first-order mineralization rate constant (k) of straw-derived carbon during the early incubation phase (Fig. 2a). Relative to the straw-only control, k values under BC-Q0 increased by 49.8% in black soil and 47.5% in fluvo-aquic soil, respectively. Cumulative straw-derived CO_2 emission by day 14 also increased systematically with PFR activity (Fig. 2b). The k values showed a significant positive correlation with ·OH production rates both in black soil (Fig. 2c, $r=0.99$, $P<0.001$) and fluvo-aquic soil (Fig. 2d, $r=0.96$, $P<0.01$). Although the response patterns were consistent across both soils, the magnitude of ·OH production and subsequent MAOM accumulation was generally greater in the black soil than in the fluvo-aquic soil.

3.3 Enhanced chemical transformation of straw-derived carbon

Dissolved organic matter (DOM) chemistry responded sensitively to biochar PFR gradients. DOM aromaticity, indicated by $SUVA_{254}$ value, was significantly higher in high-PFR treatments than in low-PFR or biochar-free treatments, particularly during the early incubation stage (Fig. 2e, f). Across treatments, $SUVA_{254}$ value increased most rapidly within the first 14 days, coinciding with elevated ·OH production and accelerated mineralization.

These results indicate that biochar PFR activity was associated not only with increased carbon turnover but also with pronounced chemical modification of straw-derived carbon during early decomposition.

3.4 Redistribution of straw-derived carbon among soil fractions

Despite enhanced early-stage mineralization, end-point carbon partitioning revealed substantial differences in the fate of straw-derived carbon among soil organic matter fractions. Increasing biochar PFR activity resulted in a significant increase in the proportion incorporated into MAOM (Fig. 3a). Under the highest PFR treatment (S + BC-Q0), straw-derived carbon accounted for 64.2 ± 2.1% of total MAOM carbon in black soil and 60.0 ± 1.4% in fluvo-aquic soil, significantly exceeding corresponding straw-only controls (59.4 ± 1.9% in black soil and 53.8 ± 2.1% in fluvo-aquic soil). Solid-state ^{13}C NMR analysis further showed that MAOM formed under high-PFR biochar treatments contained a higher proportion of aromatic carbon derived from straw compared with MAOM from low-PFR or control treatments (Fig. 3c).

3.5 Microbial community shifts along biochar PFR gradients

Microbial community composition exhibited systematic shifts along gradients of biochar PFR activity. In both soils, increasing PFR levels were associated with enrichment of bacterial taxa linked to aromatic compound degradation and oxidative stress tolerance, including members of the Sphingomonadaceae, Burkholderiaceae, and Comamonadaceae (Arkan-Ozdemir et al. 2024; Méndez et al. 2025; Táncsics et al. 2010) (Fig. 4a, b). In contrast, taxa commonly associated with rapid decomposition of labile polysaccharides, such as Streptomycetaceae and Micromonosporaceae (Yeager et al. 2017), declined in relative abundance.

Fungal communities showed parallel directional responses. The relative abundances of *Fusarium*, *Mortierella*, and *Penicillium* decreased with increasing PFR activity, whereas *Chaetomium* and members of Agaricomycetes increased (Fig. S1). These patterns were consistent across soil types, although response magnitudes differed.

Polyphenol oxidase activity increased significantly under high-PFR biochar treatments and was positively correlated with the proportion of straw-derived carbon stabilized in MAOM (Fig. 4c–e).

(See figure on next page.)

Fig. 2 Biochar PFRs accelerate early straw carbon mineralization while enhancing chemical condensation. **a** First-order mineralization rate constants (k) of straw-derived carbon during early incubation. **b** Cumulative straw-derived CO_2 ($^{13}CO_2$) released during the early phase (day 14). **c**, **d** Dose–response relationship between biochar ·OH concentration and mineralization rate constant (k) in black soil (**c**) and fluvo-aquic soil (**d**). **e**, **f** Temporal changes in dissolved organic matter aromaticity ($SUVA_{254}$) during early incubation in black soil (**e**) and fluvo-aquic soil (**f**) (***$P<0.001$; *$P<0.05$). Error bars represent standard deviations ($n=4$)

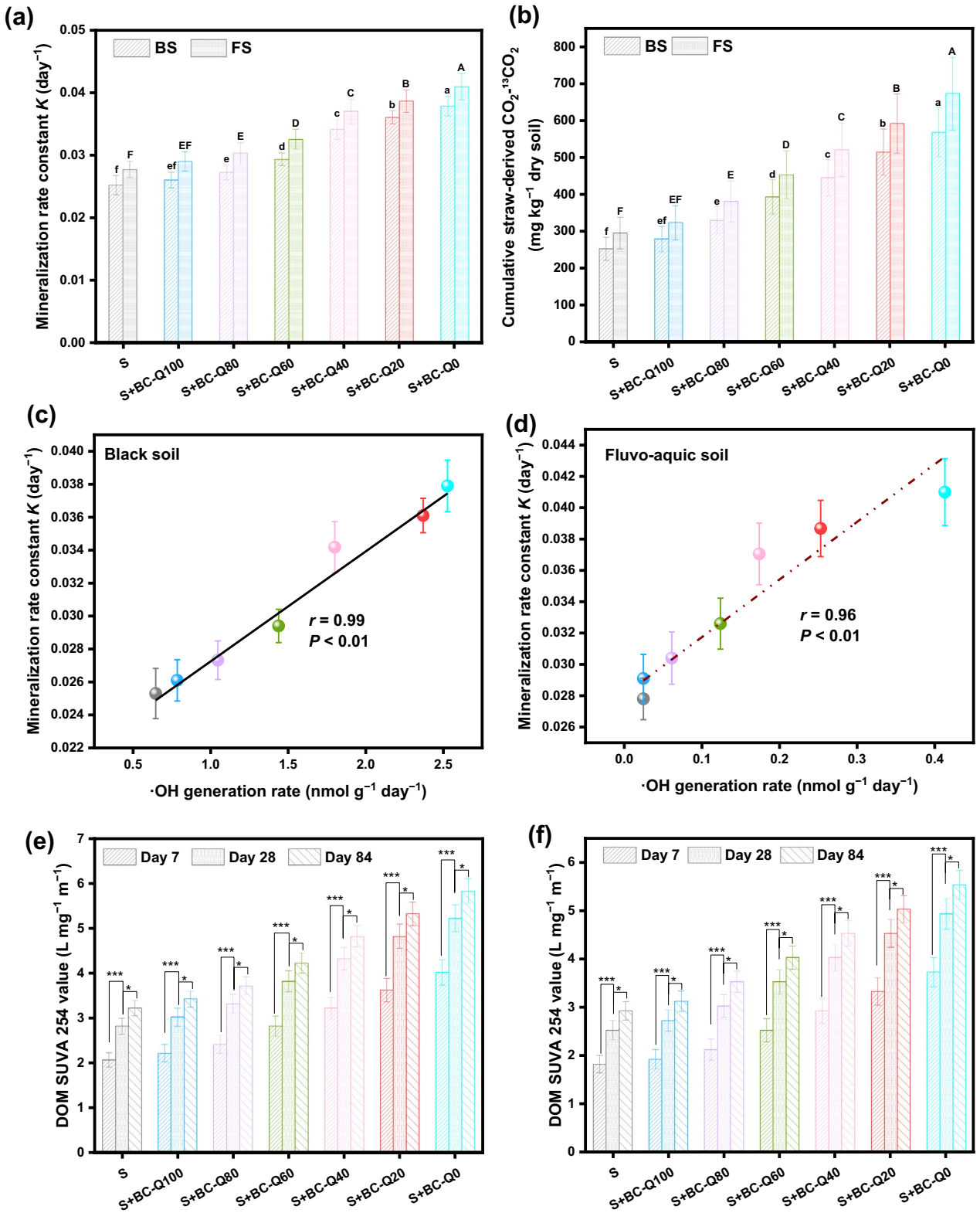
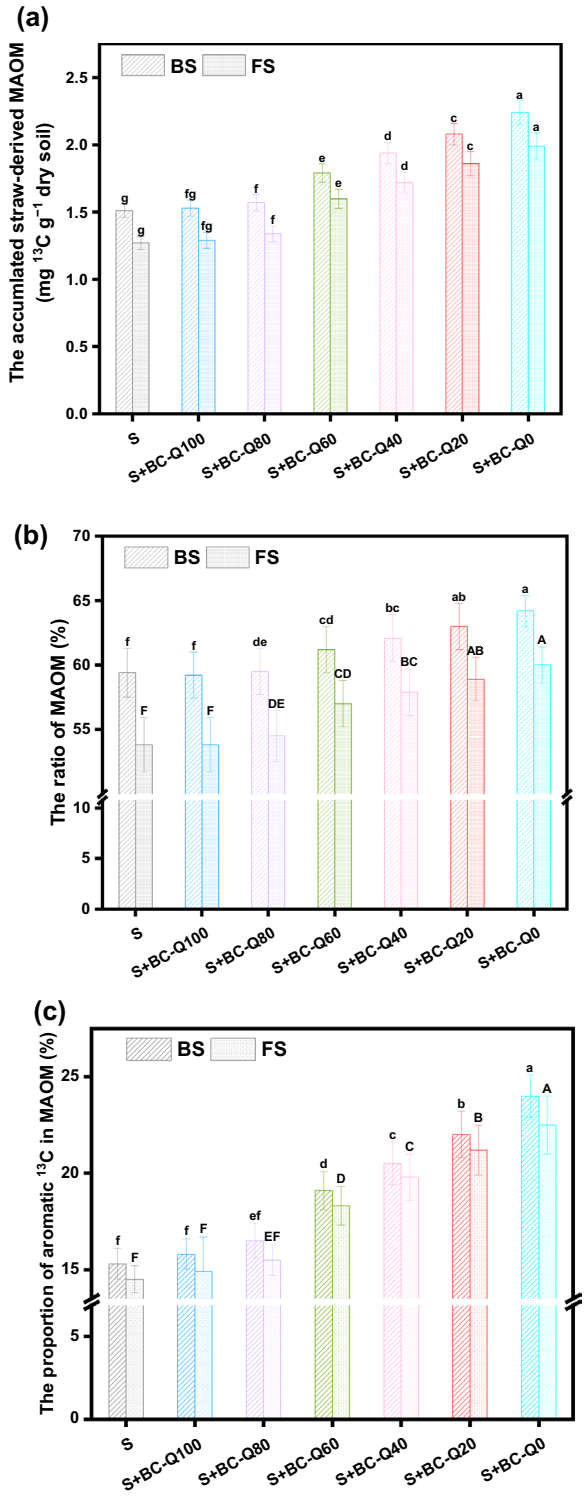


Fig. 2 (See legend on previous page.)



◀ **Fig. 3** Biochar PFRs redirect straw-derived carbon toward mineral-associated organic matter (MAOM). **a** The accumulated straw-derived carbon stabilized in the MAOM pool (^{13}C). **b** Proportion of straw-derived carbon stabilized in the MAOM pool. **c** Aromatic carbon proportion of straw-derived MAOM quantified from the aromatic resonance region (110–160 ppm) of solid-state ^{13}C NMR spectroscopy. Data are shown for black soil and fluvo-aquic soil. Error bars represent standard deviations ($n = 4$)

3.6 Structural equation modeling of coupled abiotic and biotic pathways

Structural equation modeling (SEM) integrated abiotic and biotic variables into a unified framework linking biochar PFRs to straw-derived carbon stabilization (Fig. 5). The model showed good fit (GOF = 0.83), with high explanatory power for chemical transformation ($R^2 = 0.48$), microbial functional indicators ($R^2 = 0.98$), and MAOM accumulation ($R^2 = 0.94$).

PFRs exerted a strong direct effect on ·OH production (path coefficient = 0.61, $P < 0.05$), which in turn strongly influenced chemical transformation indicators (0.70, $P < 0.05$). Chemical transformation showed a dominant effect on microbial functional responses (0.95, $P < 0.001$) and a strong total effect on straw-derived MAOM accumulation.

Overall, indirect effects accounted for the majority of the total influence of PFRs on MAOM stabilization, with pathways mediated primarily through ·OH-driven chemical transformation rather than direct microbial effects.

4 Discussion

4.1 Biochar PFRs initiate abiotic oxidation that redirects early straw carbon transformation

Residue decomposition in soil is traditionally viewed as a microbially dominated process. However, increasing evidence highlights the importance of abiotic oxidation in shaping early transformation pathways of complex plant-derived carbon (Cong et al. 2025; Li et al. 2020b; Liu et al. 2024). Our results indicate that biochar-associated PFRs function as effective drivers of abiotic oxidation, operating through pathways fundamentally distinct from microbial enzymatic processes.

During the early incubation stage, biochar PFR intensity was tightly coupled to·OH production (Fig. 1c, d) and to increased early-stage mineralization rates of straw-derived carbon (Fig. 2c, d). ·OH are highly reactive oxidants capable of oxidizing complex organic compounds and generating chemically transformed aromatic and oxygen-containing intermediates (Kim et al. 2020; Patel et al. 2021). Consistently, increasing PFR activity accelerated the initial turnover of straw-derived carbon and increased DOM aromaticity during the early incubation (Fig. 2e, f), indicating that PFR-mediated oxidation

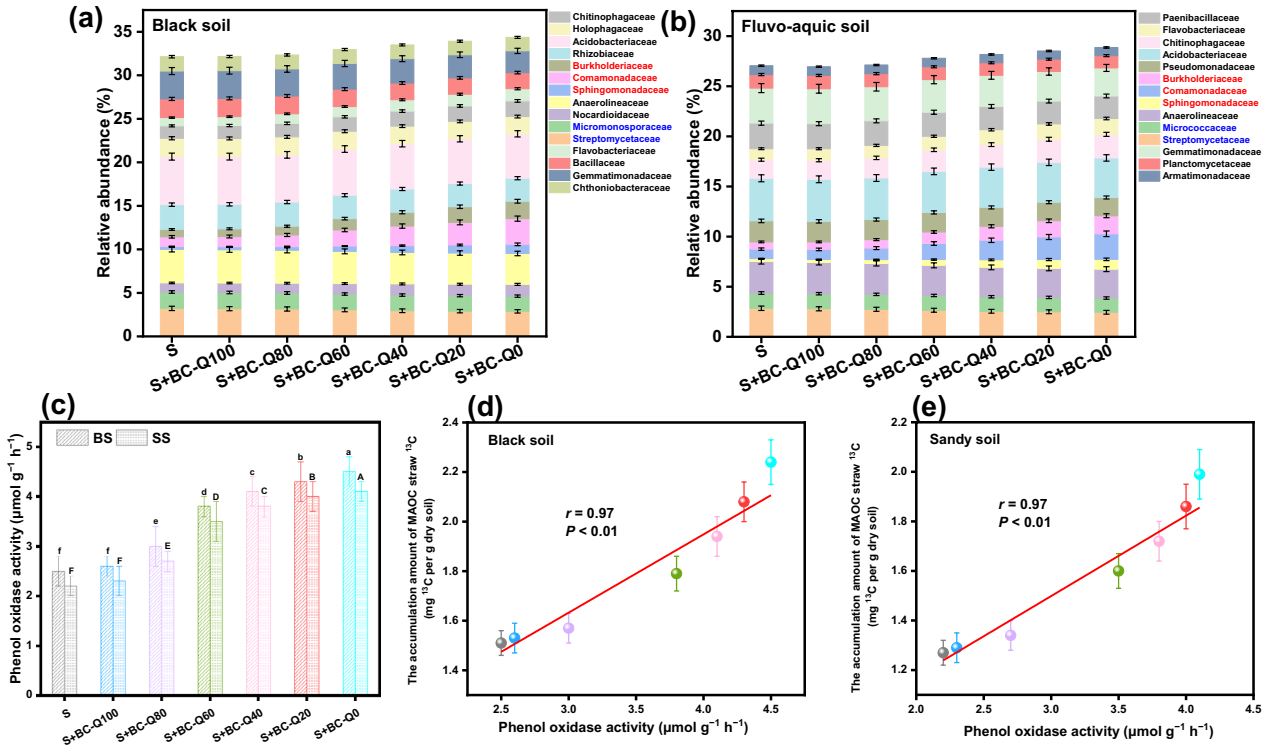


Fig. 4 Biochar PFRs reshape microbial functional indicators associated with aromatic carbon processing. **a**, **b** Relative abundances of representative bacterial taxa (family level) along the biochar PFR gradient in black soil (**a**) and fluvo-aquic soil (**b**). **c** Polyphenol oxidase activity under different biochar treatments. **d**, **e** Relationships between polyphenol oxidase activity and straw-derived carbon accumulation in MAOM in black soil (**d**) and fluvo-aquic soil (**e**). Error bars represent standard deviations ($n = 4$)

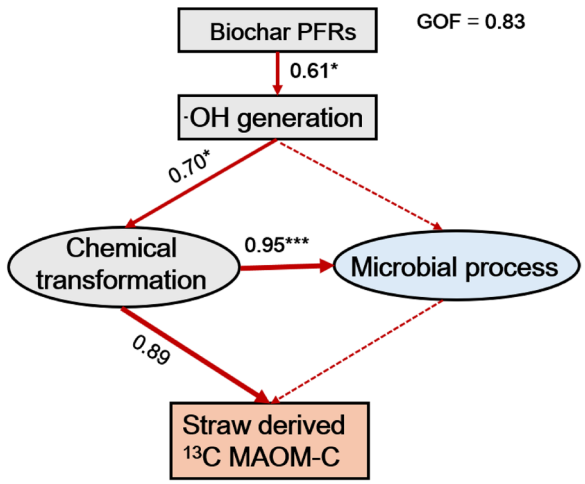


Fig. 5 Structural equation model (SEM) illustrating PFR-mediated chemo–biological coupling in soil carbon stabilization. Biochar persistent free radicals (PFRs) initiate a coupled abiotic–biotic pathway by stimulating hydroxyl radical (·OH) production, driving chemical transformation of straw-derived carbon and its preferential stabilization in mineral-associated organic matter (MAOM), with microbial functional responses acting as secondary mediators. Solid arrows indicate significant paths ($P < 0.05$); dashed arrows indicate weak or non-significant paths. Standardized path coefficients are shown

actively altered the chemical transformation of fresh residues.

Although the same mechanistic pathway was observed in both soils, the magnitude of PFR-induced ·OH production, straw carbon mineralization, and MAOM formation differed substantially, indicating that the efficiency of biochar-derived PFRs is regulated by soil physicochemical properties, particularly soil pH and native SOC. Soil pH controls the redox reactivity of environmental PFRs and ROS generation, with near neutral conditions generally favoring ·OH production over alkaline environments (Dangal et al. 2026). Moreover, soils with higher native SOC generally contain larger pools of dissolved and redox-active organic compounds, which can facilitate ROS generation and subsequent oxidative transformation (Yu et al. 2022). Consequently, the black soil (pH 6.8; SOC 28.5 g kg^{-1}) exhibited greater ·OH production and MAOM formation than the fluvo-aquic soil (pH 8.1; SOC 12.3 g kg^{-1}). These results suggest that the proposed mechanism is broadly applicable across contrasting agricultural soils, whereas the magnitude of PFR-induced carbon transformation is regulated by intrinsic soil physicochemical properties, particularly soil pH and native SOC, which together determine ROS generation and the

subsequent efficiency of substrate oxidation and MAOM formation.

Collectively, these results indicate that the early stage of straw decomposition is dominated by PFR-driven abiotic oxidation, which modifies substrate chemistry through ROS generation rather than directly stimulating microbial decomposition.

4.2 PFR-driven chemical transformation redirects straw-derived carbon toward MAOM

Following the initial oxidative stage, PFR-mediated oxidation changes the chemical trajectory of straw-derived carbon. It is reported that MAOM formation depends on the transformation of plant-derived compounds into products with enhanced mineral affinity, which facilitates their association with mineral surfaces (Sokol et al. 2019, 2022). Our results provide evidence that biochar PFRs accelerate this transformation process through an abiotic oxidation pathway. Specifically, PFR-mediated electron transfer facilitates the activation of molecular oxygen, leading to the generation of highly reactive ·OH, which may oxidize straw-derived organic matter and promote its chemical transformation (Fang et al. 2025). Among the structural components of straw, lignin exhibits higher reactivity toward radical-mediated oxidation than cellulose or hemicellulose, due to its abundant phenolic hydroxyl groups and aromatic framework that stabilize radical intermediates (Tao et al. 2022; Yang et al. 2016). ·OH preferentially attacks the β-O-4 linkages in lignin via hydrogen abstraction, generating phenolic and quinone-like fragments with high mineral affinity (Kim et al. 2020; Patel et al. 2021), increasing their potential for interaction with mineral surfaces through ligand exchange, hydrogen bonding, and organo–mineral association (Fang et al. 2025; Yang et al. 2025a). This is consistent with the rapid increase in DOM aromaticity observed in our high-PFR treatments (Fig. 2e, f), as well as the greater accumulation of straw-derived carbon in the MAOM pool and the enhanced stability of straw-derived MAOM associated with higher PFR biochars (Fig. 3). Furthermore, SEM analysis quantitatively identified chemical transformation as the primary pathway linking biochar PFR activity to straw-derived MAOM accumulation (Fig. 5).

These results indicate that ·OH produced by biochar's PFRs oxidized straw carbon into mineral-reactive intermediates, which ultimately promotes MAOM formation rather than net carbon loss. Thus, biochar's PFRs altered the chemical trajectory of straw-derived carbon by converting fresh plant residues into compounds with greater stabilization potential. The positive relationship between ·OH production, DOM aromaticity, and straw-derived MAOM contribution supported that PFR-induced oxidation selectively redirects carbon flux from rapid mineralization toward mineral-associated stabilization.

4.3 Microbial functional responses follow PFR-mediated substrate transformation

During the later stage of incubation, biochar amendment frequently alters soil microbial communities (Deshoux et al. 2023; Xu et al. 2021b). Our results indicate that the observed microbial shifts were secondary responses to PFR-mediated substrate transformation rather than the primary drivers of straw carbon decomposition.

High-PFR biochar selectively enriched bacterial taxa associated with aromatic compound metabolism and oxidative stress tolerance, while taxa specializing in rapid polysaccharide degradation declined (Fig. 4a, b). Parallel shifts were observed in fungal communities, with increased relative abundance of taxa linked to oxidative and aromatic substrate processing (Fig. S2). These compositional changes were accompanied by elevated polyphenol oxidase activity, a functional marker of oxidative carbon transformation (Fig. 4c) (Fu et al. 2025; Xu et al. 2021a).

Rather than directly initiating straw decomposition, these microbial communities likely responded to chemically modified substrates generated during PFR-mediated oxidation. This interpretation is further supported by the SEM analysis, which identified microbial functional responses as downstream processes regulated primarily by chemical transformation rather than directly by PFRs or ·OH (Fig. 5). Therefore, during the later stage of decomposition, microbial communities functioned primarily as secondary responders that further processed chemically transformed substrates, rather than initiating straw carbon transformation.

4.4 Implications, limitations, and future perspectives

Collectively, our findings support a mechanistic framework in which biochar PFRs regulate straw-derived carbon fate through a sequential chemo-biological pathway, whereby PFR-driven ·OH production initiates abiotic chemical transformation, reshapes microbial functional responses, and ultimately promotes the incorporation of straw-derived carbon into MAOM. These findings establish biochar surface redox chemistry as an important regulator of straw-derived carbon stabilization, extending the role of biochar beyond a passive carbon amendment to an active driver of soil carbon persistence.

Nevertheless, several limitations should be acknowledged. First, although chemical transformation was inferred from ROS production, DOM characteristics, and NMR analyses, neither the molecular composition of the transformation intermediates nor the relative contributions of intrinsic biochar-derived ROS, background

soil ROS, and incubation-generated radicals were directly resolved. In addition, the preferential transformation of individual straw components (e.g., cellulose, hemicellulose, and lignin) was not directly characterized. Consequently, both the specific molecular targets of PFR-mediated oxidation and the quantitative contributions of different ROS sources remain to be elucidated. Second, microbial functional responses were evaluated based on community composition and enzyme activity rather than direct measurements of functional gene expression. Finally, the proposed mechanism was established under controlled laboratory conditions using a single biochar produced from one feedstock and pyrolysis temperature. Future studies should combine component-specific analyses, high-resolution molecular characterization, multi-omics approaches, diverse biochar materials, and validation under environmentally realistic conditions, including drying–rewetting cycles, fluctuating temperatures, and long-term field experiments, to further evaluate the robustness and generality of the proposed PFR-mediated chemo-biological coupling mechanism across different soil–biochar systems.

5 Conclusions

This study demonstrates that PFRs associated with biochar actively regulate the fate of straw-derived carbon through a PFR-mediated chemo-biological coupling mechanism. Biochar PFRs stimulate abiotic oxidation, initiating chemical transformation of fresh residues into aromatic, mineral-reactive intermediates that preferentially accumulate as MAOM. Microbial functional responses subsequently mediate, rather than dominate, this stabilization pathway by favoring oxidative processing of chemically transformed substrates. These findings reframe biochar as a chemically active regulator of soil carbon pathways and provide a mechanistic basis for designing biochars to enhance soil carbon persistence.

Supplementary Information

The online version contains supplementary material available at https://doi.org/10.1007/s42773-026-00658-0.

Supplementary Material 1.

Acknowledgements
Not applicable.

Author contributions
Dan Yuan conceived and designed the study, conducted the experiments, performed data analysis and visualization, drafted the manuscript, and acquired funding. Jiao Yuan conducted the experiments, performed data analysis and visualization, and revised the manuscript. Shuping Qin supervised the research, acquired funding, and revised the manuscript. Xinliang Dong supervised the project and revised the manuscript. Xiangxiang Hao, Zhenhua Yu, Yuming Zhang, and Ping Wu revised the manuscript. All authors read and approved the final manuscript.

Funding
This work was supported by the National Key R&D Program of China (2021YFD1500400), the National Natural Science Foundation of China (42507446 and U25A20818), the Natural Science Foundation of Hebei Province (D2026503016 and D2026503009), and the Postdoctoral Project of Hebei Province (B2025005034).

Data availability
The datasets generated and/or analyzed during the current study are available from the corresponding author upon reasonable request.

Declarations

Competing interests
The authors declare that they have no competing interests.

Author details
[1]Hebei Provincial Key Laboratory of Soil Ecology, Institute of Genetics and Developmental Biology, The Chinese Academy of Sciences, 286 Huaizhong Road, Shijiazhuang 050021, Hebei, China. [2]University of Chinese Academy of Sciences, 19 A Yuquan Road, Shijingshan District, Beijing 100049, China. [3]Northeast Institute of Geography and Agroecology, Chinese Academy of Sciences, 138 Haping Road, Harbin 150081, China.

Received: 22 April 2026 Revised: 22 July 2026 Accepted: 9 September 2026
Published online: 29 October 2026

References

Alvarez R (2024) A quantitative review of the effects of residue removing on soil organic carbon in croplands. Soil Till Res 240:106098. https://doi.org/10.1016/j.still.2024.106098

Arkan-Ozdemir S, Üstüntürk-Onan M, Ilhan-Sungur E (2024) Facivitalis istanbulensis gen. nov., sp. Nov., a novel member of the family *Sphingomonadaceae* with the potential for aromatic-degradation isolated from Jet al fuel. Anton Leeuw Int J G 118:34. https://doi.org/10.1007/s10482-024-02037-w

Chacón FJ, Sánchez-Monedero MA, Lezama L, Cayuela ML (2020) Enhancing biochar redox properties through feedstock selection, metal preloading and post-pyrolysis treatments. Chem Eng J 395:125100. https://doi.org/10.1016/j.cej.2020.125100

Chang Z, Tian L, Dong J, Chen Q, Wu M, Pan B (2022) The molecular markers provide complementary information for biochar characterization before and after HNO_3/H_2SO_4 oxidation. Chemosphere 301:134422. https://doi.org/10.1016/j.chemosphere.2022.134422

Chen G, Fang Y, Van Zwieten L, Xuan Y, Tavakkoli E, Wang X, Zhang R (2021) Priming, stabilization and temperature sensitivity of native SOC is controlled by microbial responses and physicochemical properties of biochar. Soil Biol Biochem 154:108139. https://doi.org/10.1016/j.soilbio.2021.108139

Chen X, Alvarez PJJ, Masiello CA (2025) Environmentally persistent free radicals in biochar: environmental context and future research needs. Environ Sci Technol 59:11440–11454. https://doi.org/10.1021/acs.est.4c13603

Cong M, Zhang Z, Tariq A, Graciano C, Sardans J, Wang W, Gao Y, Dong X, Zhao G, Yan J, Peñuelas J, Zeng F (2025) Microbial drivers of soil organic carbon formation from aboveground residue decomposition in desert ecosystems. Appl Soil Ecol 216:106572. https://doi.org/10.1016/j.apsoil.2025.106572

Cotrufo MF, Soong JL, Horton AJ, Campbell EE, Haddix Michelle L, Wall DH, Parton WJ (2015) Formation of soil organic matter via biochemical and physical pathways of litter mass loss. Nat Geosci 8:776–779. https://doi.org/10.1038/ngeo2520

Dangal P, Kanchatryan L, Yu Q, Lomnicki SM (2026) pH-dependent activation of EPFRs and kinetics of hydroxyl radical generation. Environ Sci Technol 60:9451–9461. https://doi.org/10.1021/acs.est.6c00598

Deshoux M, Sadet-Bourgeteau S, Gentil S, Prévost-Bouré NC (2023) Effects of biochar on soil microbial communities: A meta-analysis. Sci Total Environ 902:166079. https://doi.org/10.1016/j.scitotenv.2023.166079

Dong L, Hu W, Li Q, Liu Y, Lin X, He Z, Li G (2025) Soil C mineralization and C-Fe coupling: a trade-off between Fenton reaction and microbial activity under straw mulching in banana orchards. J Environ Manage 387:125851. https://doi.org/10.1016/j.jenvman.2025.125851

Fang W, Chen Y, Zhang A, Nghiem LD, Wei Y, Johir MAH, Ding G, Xu T, Li J (2025) Reactive oxygen species (ROS)-mediated conversion of organic matter into humus: A meta-analysis on mechanisms and environmental implications. J Environ Sci. https://doi.org/10.1016/j.jes.2025.07.012

Fu Y, Xu Y, Wang Q, Van Zwieten L, Liang C, Xu J, Guggenberger G, Luo Y (2025) Deciphering the microbial players driving straw decomposition and accumulation in soil components of particulate and mineral-associated organic matter. Soil Biol Biochem 209:109871. https://doi.org/10.1016/j.soilbio.2025.109871

Fuertes AB, Arbestain MC, Sevilla M, Maciá-Agulló JA, Fiol S, López R, Smernik RJ, Aitkenhead WP, Arce F, Macías F (2010) Chemical and structural properties of carbonaceous products obtained by pyrolysis and hydrothermal carbonisation of corn stover. Soil Res 48:618. https://doi.org/10.1071/sr10010

Hao X, Han X-Z, Li N, Lei W, Chen X, Xing B (2022) Long-term grassland restoration exerts stronger impacts on the vertical distribution of labile over recalcitrant organic carbon fractions in Mollisols. Soil Sci Soc Am J 86:1444–1456. https://doi.org/10.1002/saj2.20422

Kallenbach CM, Frey SD, Grandy AS (2016) Direct evidence for microbial-derived soil organic matter formation and its ecophysiological controls. Nat Commun 7:13630. https://doi.org/10.1038/ncomms13630

Karan SK, Woolf D, Azzi ES, Sundberg C, Wood SA (2023) Potential for biochar carbon sequestration from crop residues: A global spatially explicit assessment. GCB Bioenergy 15:1424–1436. https://doi.org/10.1111/gcbb.13102

Khan K, Tewari SK, Semwal M, Verma RK (2022) Effects of aromatic crops based cropping systems and residue returning on soil CO_2 emission compared to fallow soil. J Appl Res Med Aroma 26:100351. https://doi.org/10.1016/j.jarmap.2021.100351

Kim J-Y, Moon J, Lee JH, Jin X, Choi JW (2020) Conversion of phenol intermediates into aromatic hydrocarbons over various zeolites during lignin pyrolysis. Fuel 279:118484. https://doi.org/10.1016/j.fuel.2020.118484

Lenka S, Trivedi P, Singh B, Singh BP, Pendall E, Bass A, Lenka NK (2019) Effect of crop residue addition on soil organic carbon priming as influenced by temperature and soil properties. Geoderma 347:70–79. https://doi.org/10.1016/j.geoderma.2019.03.039

Li S, Shao L, Zhang H, He P, Lu F (2020a) Quantifying the contributions of surface area and redox-active moieties to electron exchange capacities of biochar. J Hazard Mater 394:122541. https://doi.org/10.1016/j.jhazmat.2020.122541

Li Z, Song M, Li D, Ma L, Zhao B, Zhang J (2020b) Effect of long-term fertilization on decomposition of crop residues and their incorporation into microbial communities of 6-year stored soils. Biol Fertil Soils 56:25–37. https://doi.org/10.1007/s00374-019-01398-z

Liu F, Ding Y, Liu J, Latif J, Qin J, Tian S, Sun S, Guan B, Zhu K, Jia H (2024) The effect of redox fluctuation on carbon mineralization in riparian soil: an analysis of the hotspot zone of reactive oxygen species production. Water Res 265:122294. https://doi.org/10.1016/j.watres.2024.122294

Lu L, Luo Y, Jiang B, Lv JT, Meng C, Liao Y, Reid BJ, Ding F, Lu Z, Kuzyakov Y, Xu J (2022) Biochar induces mineralization of soil recalcitrant components by activation of biochar responsive bacteria groups. Soil Biol Biochem. https://doi.org/10.1016/j.soilbio.2022.108778

Ma R, Wu X, Liu Z, Yi Q, Xu M, Zheng J, Bian R, Zhang X, Pan G (2023) Biochar improves soil organic carbon stability by shaping the microbial community structures at different soil depths four years after an incorporation in a farmland soil. Curr Res Environ Sus 5:100214. https://doi.org/10.1016/j.crsust.2023.100214

Mantel S, Dondeyne S, Deckers S (2023) World reference base for soil resources (WRB). In: Goss MJ, Oliver M (eds) Reference module in earth systems and environmental sciences. Elsevier, Amsterdam

Méndez V, Sepúlveda M, Izquierdo-Fiallo K, Macaya CC, Esparza T, Báez-Matus X, Durán RE, Levicán G, Seeger M (2025) Surfing in the storm: how *Paraburkholderia* xenovorans thrives under stress during biodegradation of toxic aromatic compounds and other stressors. FEMS Microbiol Rev 49:fuaf021. https://doi.org/10.1093/femsre/fuaf021

Nazir MJ, Li G, Nazir MM, Zulfiqar F, Siddique KHM, Iqbal B, Du D (2024) Harnessing soil carbon sequestration to address climate change challenges in agriculture. Soil Till Res 237:105959. https://doi.org/10.1016/j.still.2023.105959

Patel KF, Tejnecký V, Ohno T, Bailey VL, Sleighter RL, Hatcher PG (2021) Reactive oxygen species alter chemical composition and adsorptive fractionation of soil-derived organic matter. Geoderma 384:114805. https://doi.org/10.1016/j.geoderma.2020.114805

Qin S, Wang Y, Hu C, Oenema O, Li X, Zhang Y, Dong W (2012) Yield-scaled N_2O emissions in a winter wheat–summer corn double-cropping system. Atmos Environ 55:240–244. https://doi.org/10.1016/j.atmosenv.2012.02.077

Raza S, Irshad A, Margenot A, Zamanian K, Li N, Ullah S, Mehmood K, Ajmal Khan M, Siddique N, Zhou J, Mooney SJ, Kurganova I, Zhao X, Kuzyakov Y (2024) Inorganic carbon is overlooked in global soil carbon research: a bibliometric analysis. Geoderma 443:116831. https://doi.org/10.1016/j.geoderma.2024.116831

Ruan X, Sun Y, Du W, Tang Y, Liu Q, Zhang Z, Doherty W, Frost RL, Qian G, Tsang DCW (2019) Formation, characteristics, and applications of environmentally persistent free radicals in biochars: a review. Bioresour Technol 281:457–468. https://doi.org/10.1016/j.biortech.2019.02.105

Shi L, Xia L (2024) Study on the effects of different factors on carbon pools in terrestrial ecosystems. Front Sust Dev 4:51–58. https://doi.org/10.54691/brrk1p19

Soil Survey Staff (2010) Keys to soil taxonomy, 11th edn. USDA—Natural Resources Conservation Service, Washington, DC

Sokol NW, Sanderman J, Bradford MA (2019) Pathways of mineral-associated soil organic matter formation: integrating the role of plant carbon source, chemistry, and point of entry. Glob Change Biol 25:12–24. https://doi.org/10.1111/gcb.14482

Sokol NW, Whalen ED, Jilling A, Kallenbach C, Pett-Ridge J, Georgiou K (2022) Global distribution, formation and fate of mineral-associated soil organic matter under a changing climate: a trait-based perspective. Funct Ecol 36:1411–1429. https://doi.org/10.1111/1365-2435.14040

Táncsics A, Szabó I, Baka E, Szoboszlay S, Kukolya J, Kriszt B, Márialigeti K (2010) Investigation of catechol 2,3-dioxygenase and 16S rRNA gene diversity in hypoxic, petroleum hydrocarbon contaminated groundwater. Syst Appl Microbiol 33:398–406. https://doi.org/10.1016/j.syapm.2010.08.005

Tang Z, Zhao S, Qian Y, Jia H, Gao P, Kang Y, Lichtfouse E (2021) Formation of persistent free radicals in sludge biochar by hydrothermal carbonization. Environ Chem Lett 19:2705–2712. https://doi.org/10.1007/s10311-021-01198-8

Tang H, Hu J, Li B, Liu Y, Tong WK, Yue MR, Wang J, Wang W, Gao MT, Liu N, Li J (2025) Degradation-resistant biochar improves soil organic carbon storage: Promoting autotrophic metabolism & increasing refractory organic carbon. Bioresour Technol 428:132452. https://doi.org/10.1016/j.biortech.2025.132452

Tao W, Zhang P, Li H, Yang Q, Oleszczuk P, Pan B (2022) Generation mechanism of persistent free radicals in lignocellulose-derived biochar: Roles of reducible carbonyls. Environ Sci Technol 56:10462–10472. https://doi.org/10.1021/acs.est.1c06997

Wang Y, Gu X, Huang Y, Ding Z, Chen Y, Hu X (2022) Insight into biomass feedstock on formation of biochar-bound environmentally persistent free radicals under different pyrolysis temperatures. RSC Adv 12:19318–19326. https://doi.org/10.1039/d2ra03052g

Wang Z, Luo Z, You J, Zhu X, Sui X, Ji G (2026) Synergistic application of biochar with organic fertilizer enhances soil carbon sequestration by optimizing mineral-associated organic matter formation pathway contributions. Bioresour Technol 445:134063. https://doi.org/10.1016/j.biortech.2026.134063

Weng Z, Van Zwieten L, Tavakkoli E, Rose MT, Singh BP, Joseph S, Macdonald LM, Kimber S, Morris S, Rose TJ, Archanjo BS, Tang C, Franks AE, Diao H, Schweizer S, Tobin MJ, Klein AR, Vongsvivut J, Chang SLY, Kopittke PM, Cowie A (2022) Microspectroscopic visualization of how biochar lifts the soil organic carbon ceiling. Nat Commun 13:5177. https://doi.org/10.1038/s41467-022-32819-7

Xu H, Qu Q, Chen Y, Liu G, Xue S (2021a) Responses of soil enzyme activity and soil organic carbon stability over time after cropland abandonment in different vegetation zones of the Loess Plateau of China. CATENA 196:104812. https://doi.org/10.1016/j.catena.2020.104812

Xu W, Whitman WB, Gundale MJ, Chien CC, Chiu CY (2021b) Functional response of the soil microbial community to biochar applications. GCB Bioenergy 13:269–281. https://doi.org/10.1111/gcbb.12773

Xu Y, Yu Y, Sheng J, Wang Y, Yang H, Li FM, Liu S, Kan ZR (2024) Long-term residue returning increased subsoil carbon quality in a rice-wheat cropping system. J Environ Manage 360:121088. https://doi.org/10.1016/j.jenvman.2024.121088

Yang J, Pan B, Li H, Liao S, Zhang D, Wu M, Xing B (2016) Degradation of *p*-Nitrophenol on biochars: role of persistent free radicals. Environ Sci Technol 50:694–700. https://doi.org/10.1021/acs.est.5b04042

Yang K, Jia B, Liu J, Zhu K, Qin J, Jia H (2025a) A novel perspective on the role of hydroxyl radicals in soil organic carbon mineralization within the detritusphere: stimulating C-degrading enzyme activities. Environ Sci Technol 59:5045–5055. https://doi.org/10.1021/acs.est.4c13619

Yang K, Liu J, Wang Z, Zhu K, Jia B, Yang H, Qin J, Xie J, Latif J, Liu F, Li Y, Chen N, Jia H (2025b) Spatiotemporal dynamics of reactive oxygen species in the detritusphere and their critical roles in organic carbon mineralisation. Soil Biol Biochem 202:109700. https://doi.org/10.1016/j.soilbio.2024.109700

Yeager CM, Gallegos-Graves LV, Dunbar J, Hesse CN, Daligault H, Kuske CR (2017) Polysaccharide degradation capability of actinomycetales soil isolates from a semiarid grassland of the Colorado Plateau. Appl Environ Microbiol 83:e03020-e3016. https://doi.org/10.1128/AEM.03020-16

Yu C, Lu Y, Zhang Y, Qian A, Zhang P, Tong M, Yuan S (2022) Significant contribution of solid organic matter for hydroxyl radical production during oxygenation. Environ Sci Technol 56:11878–11887. https://doi.org/10.1021/acs.est.2c02766